Advanced Materials Research Vol. 68 (2009) pp 60-68
Online available since 2009/Apr/27 at www.scientific.net

doi:10.4028/www.scientific.net/AMR.68.60

Preparation and microstructural studies of electrodeposited FeSe thin films

Kyungsik Kim[1] S.Thanikaikarasan[2,a], T.Mahalingam[2,b], S.Velumani[3,C], Taekyu Kim[4], Yong Deak Kim[1] and Rene Asomoza[3,d]

[1] Department of Electrical and Computer Engineering, College of Information Technology, Ajou University, Suwon 443 749, Republic of Korea.
[2] Department of Physics, Alagappa University, Karaikudi-630 003, Tamil Nadu,India.
[3]Department of Electrical Engineering (SEES), CINVESTAV-IPN, Col San Pedro Zacatenco, D.F.Mexico C.P.07360, Mexico.
[4] Center for Modeling and Simulation Studies, Security Management Institute, Kangnam-Ku, Seoul 135-871, Republic of Korea.

[a] s_thanikai@rediffmail.com,[b] maha51@rediffmail.com, [c]velu@cinvestav.mx, [d]rasomoza@admon.cinvestav.mx

Keywords: Thin films, FeSe, electrodeposition, crystal structure, microstructural parameters, surface morphology.

Abstract: Iron selenide (FeSe) thin films were electrodeposited onto tin oxide coated conducting glass substrates using aqueous solution mixture containing $FeSO_4$ and SeO_2 at various bath temperatures and deposition potentials. The deposited films were characterized by x-ray diffraction (XRD), scanning electron microscopy (SEM) and energy dispersive analysis by x-rays (EDX) for their structural, morphological and compositional properties. X-ray diffraction patterns revealed that the deposited films are found to be tetragonal structure with preferential orientation along (100) plane. The x-ray line profile analysis technique by the method of variance has been used to evaluate the microstructural parameters such as, crystallite size, R.M.S strain, dislocation density and stacking fault probability. The influence of bath temperature and deposition potential on the microstructual parameters was investigated. The SEM observation reveals uniform surface morphology for films deposited at higher bath temperatures. The experimental observations are discussed in detail.

1. Introduction

Thin films of iron chalcogenides are considered important technological materials because of their potential applications in photovoltaic, photodetection and opto electronic devices [1-3]. Iron chalcogenide compounds are usually prepared by several techniques such as sulphuration of iron predeposited films [4], selenization of evaporated iron thin films [1]. Iron Selenide (FeSe) thin films are usually crystallized in the tetragonal structure (PDF-03-0533) and in the hexagonal structure (PDF-75-0608). Feng et al reported the growth of FeSe thin films on GaAs substrate by low-pressure metal organic chemical vapor deposition (LP-MOCVD) and studied their structural, compositional and morphological properties [5]. The magnetic properties of FeSe thin films prepared on GaAs substrate by molecular beam epitaxy was reported by Takemura et al [6]. Ouertani et al studied the structural, morphological and electrical properties of iron diselenide thin films prepared by soft selenization of iron oxide thin films [7].

Among various thin film growing techniques, electrodeposition provide numerous advantages including low temperature processing, arbitrary shape, controllable film thickness and morphology , composition and easy process to obtain good quality films [8-9]. Most of the research reports on FeSe thin films deal with qualitative observations of film preparation, characterization, composition and crystallite size variation with deposition parameters.

A detailed quantitative determination of the different microstructural parameters like crystallite size, R.M.S strain, dislocation density and stacking fault probability have not yet been studied and reported for electrosynthesized FeSe thin films. Knowledge of microstructural analysis may provide valuable informations on the optimum growth conditions of the films. X-ray diffraction study based on precise measurements upon the position broadening and shape of x-ray profiles on polycrystalline thin film gives informations about the microstructural parameters which characterizes the microstructural variations in the films. The microstructural parameters such as crystallite size, R.M.S strain, dislocation density and stacking fault probability are expected to influence the physico chemical properties of electrodeposited FeSe thin films. Moreover, the reduction of stress, dislocation density and increase in grain size of FeSe thin films is of immense need for optoelectronic applications. To our knowledge no report is available for tetragonal FeSe thin film growth by electrodeposition technique owing to their wide difference in electrochemical properties and difficulty to obtain FeSe thin films. The objective of the present study is to prepare FeSe thin films on tin oxide (SnO_2) coated conducting glass substrates by electrodeposition technique. The deposited films were subjected to x-ray diffraction, scanning electron microscope, energy dispersive analysis by x-rays for studying their structural, morphological and compositional behaviour. X-ray line profile analysis technique by the method of variance has been used to evaluate the microstctural parameters such as crystallite size, R.M.S strain, dislocation density and stacking fault probability. The dependence of microstructural parameters with bath temperature and deposition potentials were studied and discussed.

2. Experimental Details

FeSe thin films were prepared by electrodeposition technique on tin oxide coated conducting glass substrates by the potentiostatic mode using an EG & G, Princeton Applied Research Potentiostat/Galvanostat, Model 362, USA. Control of the deposition process is in principle easier in the potentiostatic mode, since the growth process shows a form of cathodic inhibition. Nevertheless, this growth mode can be applied reliable only if low resistance cathodic substrates are used. The normal three electrode system was used to obtain FeSe thin films with tin oxide coated glass substrate (sheet resistance 20 Ω/□) as working electrode, graphite rod as counter electrode and a saturated calomel electrode (SCE) as reference electrode, respectively. The saturated calomel electrode was introduced into the solution by a luggin capillary whose tip was placed as close as possible to the working electrode. All the experimental potentials are referred to this electrode. Before use, tin conductive oxide substrates were treated for 15 minutes ultrasonically in a bath of isopropanol and then rinsed with acetone. The electrolytic bath consists of 0.02 M $FeSO_4$ and 0.001 M SeO_2 with solution pH maintained at 2.0±0.1. The bath temperature and deposition potential was kept in the range between 30 to 80^0C and -600 to -900 mV versus SCE. The optimized deposition conditions to obtain good quality films are: (i) Electrolyte concentration: 0.02 M $FeSO_4$ and 0.001 M SeO_2, (ii) Bath temperature: 80^0C (iii) Deposition potential:-900 mV Vs SCE (iv) solution pH: 2.0±0.1.

X-ray diffraction data of the electrodeposited FeSe thin films were recorded using a JEOL-JDX 8030 diffractometer with Cuk_α radiation (λ=1.5418 Å). Calculation of crystallite size and R.M.S strain were made using an x-ray line profile analysis. Dislocation densities are calculated from crystallite size and R.M.S strain values using equation (4) as the method given by Williamson and Smallman [14]. The stacking fault probability was calculated from the peak shit using equation (5) given by Warren and Warekois [13]. Surface morphology and film composition was analyzed using an energy dispersive analysis by x-rays set up attached with scanning electron microscope (Philips Model XL 30), respectively.

3. Results and Discussion

3.1. Structural studies

X-ray diffraction studies were carried out in order to determine the crystalline nature of the deposited films. Using x-ray diffraction data the interplanar spacing 'd' was calculated using the relation (1).

$$d_{hkl} = \frac{\lambda}{2\sin\theta} \quad (1)$$

Fig. 1 shows the x-ray diffraction pattern of FeSe thin films deposited at various bath temperatures from 30 to 80^0C at a deposition potential of -900 mV versus SCE. XRD patterns revealed that the deposited films possess polycrystalline in nature with tetragonal structure with lattice constants (a=3.74 Å; c=5.50Å). The diffraction peaks of FeSe are found at 2θ values of 28.51, 32.27, 33.47, 37.27, 47.32, 49.12, 51.07, 55.42, 57.02,59.22, 67.67, 70.52, 76.52 corresponding to the lattice planes (100), (002), (110), (111), (112), (003), (201), (103), (211), (202), (004), (220) and (211), respectively. The'd' values calculated using equation (1) confirm well with available JCPDS standard for FeSe [10]. It is observed from Fig.1 that the crystallites are preferentially oriented along (110) plane. It is also observed that some new peaks of FeSe are begins to appear while increasing bath temperature from 30 to 80^0C. If the bath temperature is increased the intensity of preferential peak increases upto 80^0C, afterwards it slightly decreases not shown in Fig.1.

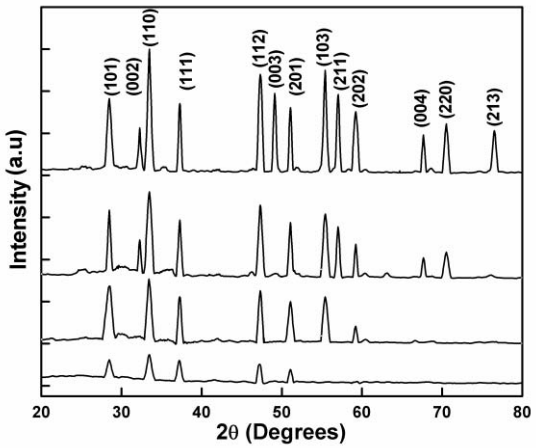

Fig. 1. X-ray diffraction pattern of FeSe thin films electrodeposited at various bath temperatures (a) 30^0 (b) 50^0C (c) 70^0C (d) 80^0C.

Hence, the bath temperature is fixed as 80^0C for further depositions. The average crystallite size of the deposited films can be determined by Full Width at Half Maximum (FWHM) using Debye-Scherrer's formula [8].

$$D = \frac{0.9\lambda}{\beta\cos\theta_B} \quad (2)$$

where β is the Full Width at Half Maximum of the peak in radians, λ is the wavelength of CuK_α target (λ=0.15418 nm), θ_B is the Bragg diffraction angle at peak position in degrees. The sizes of the crystallites are found to be in the range between 19 and 40 nm.

3.2. Line Profiles and variance analysis

Pure diffraction profiles of lines in X-ray diffraction patterns are generally due to convolution of various factors like crystallite size, R.M.S strain and stacking faults. For the calculation of crystallite size and R.M.S strain, the line profiles were subjected to variance analysis suggested by the method given by Mitra [11]. An aggregate of distorted crystallites as a measure of the particle size and strain could affect the variance of the x-ray diffraction line profiles. Since the method is sensitive to variation near the tails of the peaks, a careful adjustment of the background was carried out following the method of Mitra and Misra [12].

Since the variances are additive, the profiles were corrected for instrumental broadening by substracting the variance of the corresponding profile of standard well annealed FeSe sample. If it is assumed that the broadening of the x-ray line is due to crystallite size and strain only, the variance can be written as

$$W_{2\theta} = \left[\frac{\lambda\sigma}{2\pi^2 PCos\theta}\right] + \left[4\tan^2\theta < e^2 >\right] \quad (3)$$

where λ is the wavelength of x-rays used, σ the angular range over which the intensity distribution is appreciable, P the crystallite size, θ the Bragg angle and $<e^2>^{1/2}$ is the mean squared strain. However, variance is a range sensitive parameter and consequently depends on the background level which has a marked influence on the range to be selected for integration. In fact, it is found that the diffraction profiles approach zero, rather asymptotically, following an inverse square law. For such a function varying inversely as the square of the distance from the mean, the variance can be written as W = Kσ + C, where K and C are constants and are dependent on the physical conditions of the sample and the geometrical factors. Dislocation density is defined as the length of dislocation line per unit volume of the crystal [13]. Williamson and Smallman [14] suggested one method to calculate the dislocation density as

$$\rho = \left[\frac{(3nK/F)^{1/2}\ \langle e^2\rangle^{1/2}}{bP}\right] \quad (4)$$

where P is the crystallite size, $<e^2>^{1/2}$ is the R.M.S strain, b the Burgers vector, n the number of dislocations on each face of the particle, K the constant depending on the strain distribution and F is an interaction parameter. For Cauchy strain profiles the value of K is about 25, whereas for Gaussian strain profiles it is nearly 4. In the absence of extensive polygonization, dislocation density can be calculated from the above equation (4) by assuming n≈F, b=d the interplanar spacing and K= 4. Now the equation (4) reduces to

$$\rho = \frac{\sqrt{12}\langle e^2\rangle^{1/2}}{dP} \quad (4)$$

The stacking fault probability α is the fraction of layers undergoing stacking sequence faults in a given crystal and hence one fault is expected to be found in 1/α layers. The presence of stacking faults gives rise to a shift in the peak position of different reflections with respect to ideal positions of a fault-free, well annealed sample. Four typical experimental profiles showing the peak shift for tetragonal (110) reflection of FeSe films prepared at different bath temperatures with respect to a well annealed bulk sample reference is shown in Fig. 2.

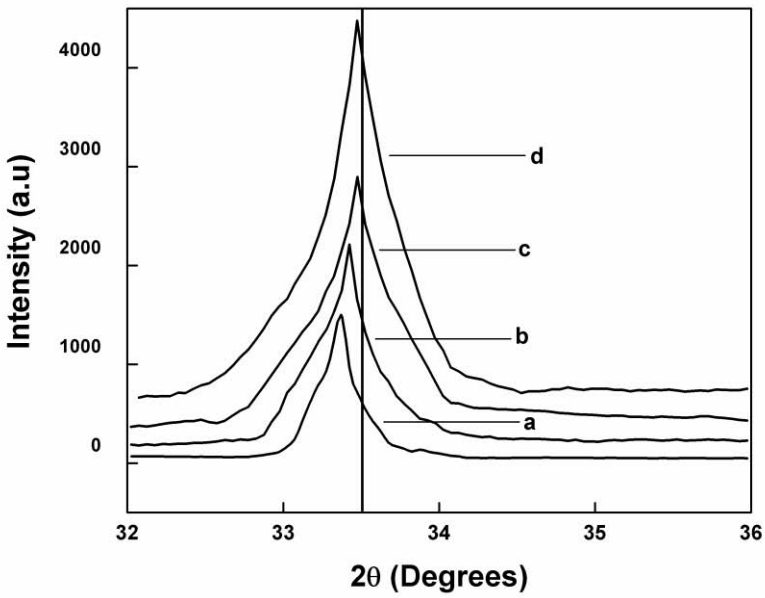

Fig. 2. X-ray diffraction profile showing the peak shift and line broadening (a) 30^0C (b) 50^0C (c) 70^0C (d) 80^0C.

A well annealed powder sample reference is used to compare the shift in the peak position of different reflections and hence to evaluate the microstructural parameters. The relation connecting stacking fault probability (α) with peak shift Δ (2θ) was given by Warren and Warekois [13]. The stacking fault probability (α) is given by

$$\alpha = \left[\frac{2\pi^2}{45\sqrt{3}}\right]\left[\frac{\Delta(2\theta)}{\tan\theta_{002}}\right] \qquad (5)$$

From the above expression (5) the stacking fault probability was calculated by measuring the peak shift with the well annealed sample.

3.3. Microstrucutral analysis

X-ray diffraction patterns of FeSe thin films deposited at various bath temperatures between 30 and 80^0C were recorded. Using FWHM data and Debye-Scherrer equation the crystallite size of the deposited films were calculated. The variation of crystallite size and R.M.S strain with bath temperature for FeSe film is shown in Fig. 3a

It is observed from Fig. 3a that the crystallite size increases gradually with bath temperature and attained a maximum value for films prepared at bath temperature of 80^0C. On the other hand, the R.M.S strain decreases with increase of bath temperature and attained a minimum value at bath temperature of 80^0C. When the bath temperature increases, large number of Fe and Se ions gets adsorbed on the substrate which leads to crystallization. This effect is more predominant at higher bath temperature which leads to a maximum value of crystallite size for films deposited at 80^0C. Due to the increase in crystallite size with bath temperature the defects in the lattice is reduced which in turn reduces the R.M.S strain.

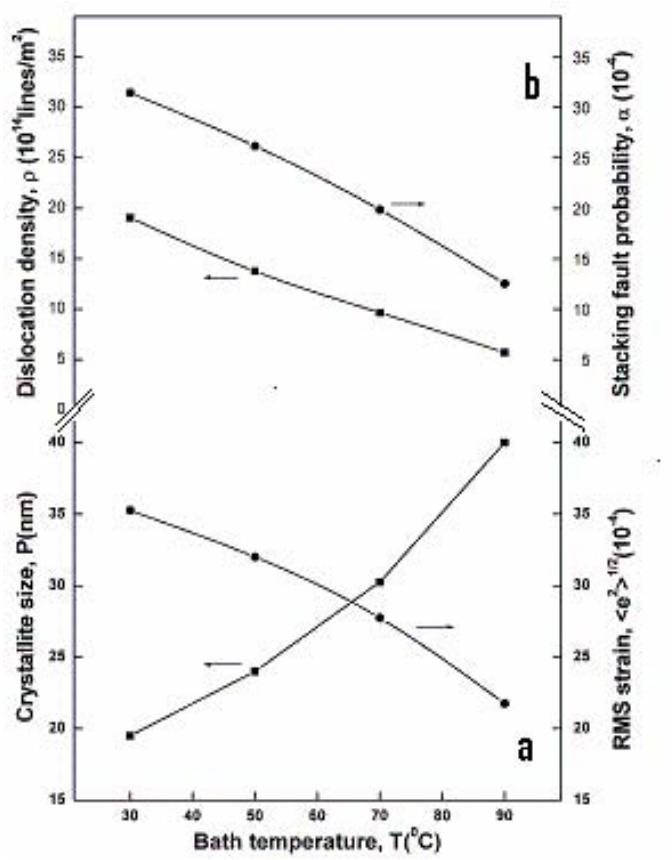

Fig. 3a. Variation of crystallite size and R.M.S strain with temperature for FeSe thin films.
Fig. 3b.Variation of dislocation density and stacking fault probability with bath temperature for FeSe thin films.

The variation of dislocation density and stacking fault probability with bath temperature is shown in Fig. 3b. It is observed from Fig. 3b that the dislocation density and stacking fault probability are found to decrease with increase of bath temperature and minimum values are obtained for films deposited at bath temperature of 80^0C. Due to the release of stress built-up in the layers, the variation of interplanar spacing decreases which finally leads to a decrease in stacking fault probability for films deposited at a bath temperature of 80^0C. The variation of microstructural parameters with bath temperature indicates that R.M.S strain, dislocation density, stacking fault probability decreases, whereas the crystallite size increases. Similar functional dependency of microstrucutral parameters with bath temperature for electrodeposited ZnTe films have been reported by Mahalingam et al. [15]. The variation of microstructural parameters with deposition potential for electrodeposited FeSe thin films were studied and reported (Fig. 4a).

It is observed from Fig.4a that the maximum value of crystallite size and minimum value of R.M.S strain were obtained for films prepared at a deposition potential of -900 mV versus SCE. Fig. 4b shows the variation of dislocation density and stacking fault probability with deposition potential for FeSe thin films prepared at various deposition potentials. It is observed Fig. 4b that the dislocation density and stacking fault probability are found to decrease while decreasing the deposition potential upto -900 mV versus SCE and minimum values are obtained for films obtained at deposition potential of -900 mV versus SCE. Similar behaviour is exhibited for Cu_2O films have been reported earlier [16].

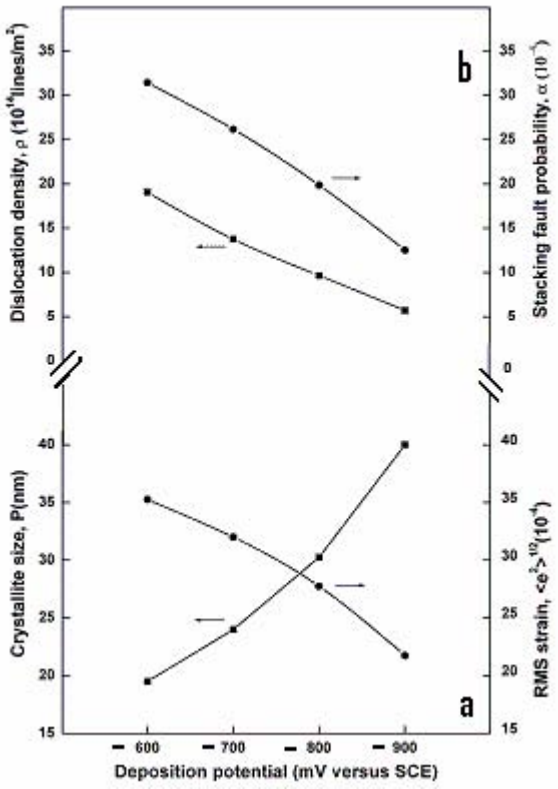

Fig. 4a.Variation of crystallite size and R.M.S strain with deposition potential for FeSe thin films.
Fig. 4b.Variation of dislocation density and stacking fault probability with deposition potential for FeSe thin films.

3.4. Morphological and Compositional analysis

The surface morphology of FeSe thin films was analyzed using scanning electron microscopy.

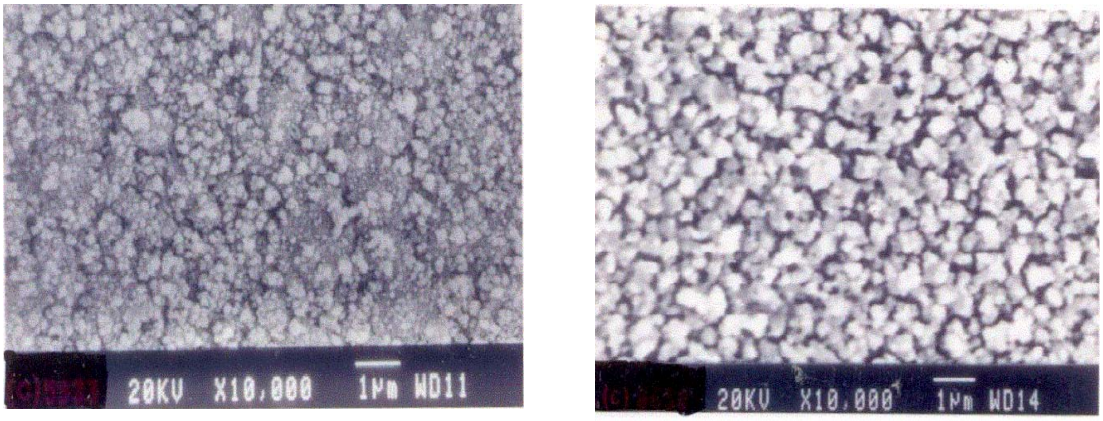

Fig. 5.a, b.SEM picture of typical FeSe thin films electrodeposited at different bath temperatures (a) 30^0C (left) b) 80^0C.(right)

Fig. 5.a,b shows the surface morphology of FeSe thin films obtained at bath temperature of 30 and 80^0C. It is observed from Fig. 5a, that the films deposited at 30^0C appeared to be non-uniform with smaller grains and exhibits coarsed like structure. Increase in bath temperature results increase in cathodic polarization. This results increase in nucleation over growth and the film surface is observed to be uniform with more compact structure (Fig. 5b).An increase in crystallite size with

bath temperature is evidenced from SEM picture. The average sizes of the grains are found to be in the range between 0.25 and 0.66 μm.The quantitative analysis of FeSe electrodeposits was performed with an aim to determine the relationship between different bath temperatures and film composition. After etching the film surface, a quantitative determination of FeSe electrodeposits was made by energy dispersive analysis by x-rays set up attached with scanning electron microscope.

The variation of Fe, Se content for FeSe thin films prepared at various bath temperatures are shown in Fig. 6.

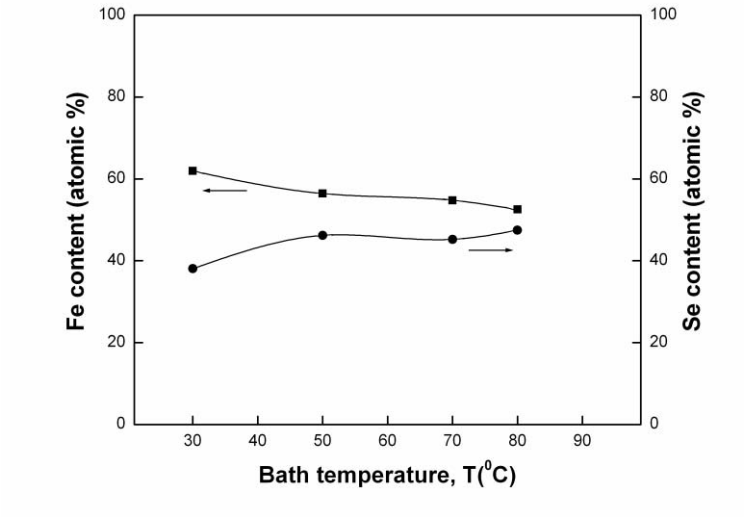

Fig. 6. Variation of Fe and Se content with bath temperature for FeSe thin films.

It is observed from Fig. 6, that the content of Fe decreased and the content of Se increased while increasing bath temperature from 30^0C to 80^0C, afterwards the content of Se slightly decreases. This observation is also evidenced by the improvement of tetragonal FeSe phase which is revealed from x-ray diffraction analysis. The atomic molar ratio of Fe: Se for FeSe thin film obtained at bath temperature of 80^0C is found to 52.55:47.45 and is nearly 1:1. This result is consistent with x-ray diffraction analysis of the sample with phase correspond to FeSe. Similar result was obtained for FeSe thin film prepared by low pressure metal organic chemical vapor deposition [5].

4. Conclusion

FeSe thin films were electrodeposited on tin oxide coated conducting glass substrates at various bath temperatures and deposition potentials. The X-ray diffraction pattern reveals tetragonal structure with preferential orientation along (110) plane. X-ray line broadening studies are carried out for films obtained at various bath temperatures and deposition potential. The microstructural parameters for FeSe thin films were evaluated and they are found to depend upon bath temperature and deposition potential. The R.M.S strains, dislocation density, stacking fault probability are found to decrease with bath temperature and deposition potential, whereas the crystallite size increases.

It is observed that microstructral parameters exhibits monotonic variation with bath temperature (30-80)^{0}C and deposition potential - (500-900) mV versus SCE in the measurement ranges. EDX analysis shows that stoichiometric films of good quality are obtained for films prepared at bath temperature of 80^0C and at a deposition potential of -900 mV versus SCE. Surface morphology reveals smooth surface for films prepared at higher bath temperature and lower deposition potential.

References

[1]. N.Hamdadou, J.C.Bernede, A.Khelil: Journal of Crystal.Growth Vol.241 (2002) p.313.

[2]. N.Hamdadou, A.Khelil, M.Morsli, J.C.Bernede: Vacuum Vol.77 (2005) p.151.

[3]. T.Harada: Journal of Physical Society of Japan Vol.67 (1998) 1352.

[4]. N.Hamdadou, A.Khelil, J.C.Bernede: Materials Chemistry and.PhysicsVol.78 (2003) p.591.

[5]. Q.J.Feng, D.Z.Shen, J.Y.Zhang, C.X.Shan, Y.M.Lu, Y.C.Liu, X.W.Fan: Journal of Magnetism and Magnetic Materials Vol.279 (2004) p.435.

[6]. Y.Takemura, N.Honda, T.Takahashi, H.Suto, K.Kakuno: Journal of Magnetism and Magnetic Materials Vol.177 (1998) p.1319.

[7]. B.Ouertani, J.Ouerfelli, M.Saadoun, B.Bessais, H.Ezzaouia, J.C.Bernede: Solar Energy.

[8]. T.Mahalingam, S.Thanikaikarasan, M.Raja, C.Sanjeeviraja, Soonil Lee, Hosun Moon, Yong Deak Kim and P.J.Sebastian Journal of New Materials for Electrochemical Systems Vol.10 (2007) p.35.

[9]. Han Joon Kwon, S.Thanikaikarasan, Thaiyan Mahalingam, Kyung Ho Park, C.Sanjeeviraja, Yong Deak Kim: Journal of Materials Science: Materials in Electronics Vol.19 (2008) p.1086.

[10] JCPDS Diffraction Data Card No.03-053.

[11]. G.B.Mitra: Acta Crystallography Vol.17 (1964) p.765.

[12]. G.B.Mitra, N.K.Misra: Britain Journal of Applied Physics Vol.17 (1966) p.1319.

[13]. B.E.Warren, E.P.Warekois: Acta Metallurgy Vol.3 (1955) p.473.

[14]. G.K.Williamson, R.E.Smallman: Philosophical Magazine Vol.1 (1956) p.34.

[15]. T.Mahalingam, V.S.John, G.Ravi, P.J.Sebastian: Crystal Research Technology Vol.37 (2002) p.329.

[16]. T.Mahalingam, J.S.P.Chitra, J.P.Chu, P.J.Sebastian: Materials Letters Vol.58 (2004) p.1802.

Advances in Semiconducting Materials
doi:10.4028/www.scientific.net/AMR.68

Preparation and Microstructural Studies of Electrodeposited FeSe Thin Films
doi:10.4028/www.scientific.net/AMR.68.60

References

[1]. N.Hamdadou, J.C.Bernede, A.Khelil: Journal of Crystal.Growth Vol.241 (2002) p.313. doi:10.1016/S0022-0248(02)01250-2

[2]. N.Hamdadou, A.Khelil, M.Morsli, J.C.Bernede: Vacuum Vol.77 (2005) p.151. doi:10.1016/j.vacuum.2004.08.014

[3]. T.Harada: Journal of Physical Society of Japan Vol.67 (1998) 1352. doi:10.1143/JPSJ.67.1352

[4]. N.Hamdadou, A.Khelil, J.C.Bernede: Materials Chemistry and.PhysicsVol.78 (2003) p.591.

[5]. Q.J.Feng, D.Z.Shen, J.Y.Zhang, C.X.Shan, Y.M.Lu, Y.C.Liu, X.W.Fan: Journal of Magnetism and Magnetic Materials Vol.279 (2004) p.435. doi:10.1016/j.jmmm.2004.02.030

[6]. Y.Takemura, N.Honda, T.Takahashi, H.Suto, K.Kakuno: Journal of Magnetism and Magnetic Materials Vol.177 (1998) p.1319. doi:10.1016/S0304-8853(97)00514-3

[7]. B.Ouertani, J.Ouerfelli, M.Saadoun, B.Bessais, H.Ezzaouia, J.C.Bernede: Solar Energy.

[8]. T.Mahalingam, S.Thanikaikarasan, M.Raja, C.Sanjeeviraja, Soonil Lee, Hosun Moon, Yong Deak Kim and P.J.Sebastian Journal of New Materials for Electrochemical Systems Vol.10 (2007) p.35.

[9]. Han Joon Kwon, S.Thanikaikarasan, Thaiyan Mahalingam, Kyung Ho Park, C.Sanjeeviraja, Yong Deak Kim: Journal of Materials Science: Materials in Electronics Vol.19 (2008) p.1086.

[10] JCPDS Diffraction Data Card No.03-053.

[11]. G.B.Mitra: Acta Crystallography Vol.17 (1964) p.765. doi:10.1107/S0365110X6400192X

[12]. G.B.Mitra, N.K.Misra: Britain Journal of Applied Physics Vol.17 (1966) p.1319. doi:10.1088/0508-3443/17/10/310

[13]. B.E.Warren, E.P.Warekois: Acta Metallurgy Vol.3 (1955) p.473. doi:10.1016/0001-6160(55)90138-3

[14]. G.K.Williamson, R.E.Smallman: Philosophical Magazine Vol.1 (1956) p.34. doi:10.1080/14786435608238074

[15]. T.Mahalingam, V.S.John, G.Ravi, P.J.Sebastian: Crystal Research Technology Vol.37 (2002) p.329. doi:10.1002/1521-4079(200204)37:4<329::AID-CRAT329>3.0.CO;2-U

[16]. T.Mahalingam, J.S.P.Chitra, J.P.Chu, P.J.Sebastian: Materials Letters Vol.58 (2004) p.1802. doi:10.1016/j.matlet.2003.10.055